Computer Vision and Image Understanding **86,** 171–190 (2002)
doi:10.1006/cviu.2002.0974

Fuzzy Distance Transform: Theory, Algorithms, and Applications

Punam K. Saha

Medical Image Processing Group, Department of Radiology, University of Pennsylvania, Fourth Floor, Blockley Hall, 423 Guardian Drive, Philadelphia, Pennsylvania 19104-6021

Felix W. Wehrli

Laboratory for Structural NMR, Department of Radiology, University of Pennsylvania Health System, 3400 Spruce Street, Philadelphia, Pennsylvania 19104

and

Bryon R. Gomberg

Department of Bio-engineering, University of Pennsylvania Health System, 3400 Spruce Street, Philadelphia, Pennsylvania 19104

Received November 5, 2001; accepted September 27, 2002

This paper describes the theory and algorithms of distance transform for fuzzy subsets, called fuzzy distance transform (FDT). The notion of fuzzy distance is formulated by first defining the length of a path on a fuzzy subset and then finding the infimum of the lengths of all paths between two points. The length of a path π in a fuzzy subset of the n-dimensional continuous space $\Re^n$ is defined as the integral of fuzzy membership values along π. Generally, there are infinitely many paths between any two points in a fuzzy subset and it is shown that the shortest one may not exist. The fuzzy distance between two points is defined as the infimum of the lengths of all paths between them. It is demonstrated that, unlike in hard convex sets, the shortest path (when it exists) between two points in a fuzzy convex subset is not necessarily a straight line segment. For any positive number $\theta \leq 1$, the θ-support of a fuzzy subset is the set of all points in $\Re^n$ with membership values greater than or equal to θ. It is shown that, for any fuzzy subset, for any nonzero $\theta \leq 1$, fuzzy distance is a metric for the interior of its θ-support. It is also shown that, for any smooth fuzzy subset, fuzzy distance is a metric for the interior of its 0-support (referred to as *support*). FDT is defined as a process on a fuzzy subset that assigns to a point its fuzzy distance from the complement of the support. The theoretical framework of FDT in continuous space is extended to digital cubic spaces and it is shown that for any fuzzy digital object, fuzzy distance is a metric for the support of the object. A

1077-3142/02 $35.00

dynamic programming-based algorithm is presented for computing FDT of a fuzzy digital object. It is shown that the algorithm terminates in a finite number of steps and when it does so, it correctly computes FDT. Several potential applications of fuzzy distance transform in medical imaging are presented. Among these are the quantification of blood vessels and trabecular bone thickness in the regime of limited special resolution where these objects become fuzzy.

Key Words: distance transform; fuzzy subset; adjacency; path; fuzzy distance; metric; dynamic programming.

1. INTRODUCTION

Effective tools for object shape analysis are important and useful in many imaging applications including medical ones. One such popular and widely used tool is the distance transform (DT) [1–4] of an object. For a hard (binary) object, DT is a process that assigns a value at each location within the object that is simply the shortest distance between that location and the complement of the object. However, this notion of hard DT cannot be applied on fuzzy objects [5–7] in a meaningful way. The notion of DT for fuzzy objects, called fuzzy distance transform (FDT), becomes more important in many imaging applications because we often deal with situations with data inaccuracies, graded object compositions, or limited image resolution (on the order of an object's structure size). In general, FDT will be useful, among others, in feature extraction [8], local thickness or scale computation [9, 10], skeletonization [11–13], and morphological [14] and shape-based object analyses [15]. In particular, FDT may be useful in fault detection in integrated circuit chips or in computer motherboard circuits, analysis of the dynamics of hurricane, etc. FDT will be useful in many medical imaging applications such as computation of local thickness of trabecular bone or of vessels, or morphology-based separation of anatomic structures having similar intensities, e.g., artery–vein separation. In this paper, we develop the theoretical and the algorithmic framework for FDT in both continuous and digital spaces, study its properties, present a dynamic programming-based algorithm to compute FDT for fuzzy digital objects, and illustrate preliminary results.

Over the past few decades, the notion of DT has popularly been applied for hard objects only. Most DT methods approximate the global Euclidean distance by propagating local distances between neighboring pixels. As observed in [4], this simple yet fundamental idea was first presented by Rosenfeld and Pfaltz [16] in 1966. In [1], they discussed different digital distance functions including city blocks and chess board distances and described how they can be mixed to create octagonal DTs that are better approximations of the Euclidean distances. Okabe, Toriwaki, and Fukumara [17] investigated these issues in 3D; this was independently discovered and illustrated in [3]. In [2], Danielsson described how to reasonably compute the true Euclidean DT in digital spaces, including the 3D case. Ragnemalm [18] presented Euclidean DT methods in arbitrary dimensions. Borgefors [3, 4, 15, 19] extensively studied DTs for hard 3D objects. In [3], she presented many types of DTs including the popular algorithm that computes DT by using different local step lengths for different types of neighbors. Also, she presented the integer-valued approximation of the optimal local step lengths. Variations of this method were presented in [20, 21]. In [4], Borgefors studied the geometry and equations of 3D DT and presented a two-pass raster scan algorithm for computing approximate Euclidean distance transform. The notion of

gray-weighted distance was introduced by Rutovitz [22] in the 1960s and was used by Levi and Montanari [23] in 1970 to define a gray-weighted skeleton. These concepts were summarized by Rosenfeld and Kak [24] in an exercise (see pp. 213–214). Mordeson and Nair [25] described different ways of defining path lengths in a fuzzy graph.

In this paper, we develop the theoretical framework of FDT in the n-dimensional continuous space $\Re^n$. Let us consider a path π over a fuzzy subset of $\Re^n$. Unlike the case of hard sets, the membership values of the points through which π passes need to be considered to determine its length. More specifically, the length of π is the integral of fuzzy membership values along π. Generally, there are infinitely many paths in a fuzzy subset between any two points $x, y \in \Re^n$ and it is demonstrated that, often, it is not possible to find one shortest path. The fuzzy distance between two points $x, y \in \Re^n$ is defined as the infimum [26] of the lengths of all paths between them. It is illustrated that, unlike the case of hard convex sets, the shortest path (when it exists) between two points in a fuzzy convex subset is not necessarily a straight line. For any positive number $\theta \leq 1$, the θ-support of a fuzzy subset is the set of all points in $\Re^n$ with membership values greater than or equal to θ. It is shown that for any fuzzy subset, for any nonzero $\theta \leq 1$, fuzzy distance is a metric for the interior of its θ-support. It is also shown that, for any smooth fuzzy subset, fuzzy distance is a metric for the interior of its 0-support (referred to as *support*). FDT is defined as a process on a fuzzy subset that assigns to a point its fuzzy distance from the complement of the support. The theoretical framework of FDT in the continuous space is extended to cubic digital spaces and it is shown that for any fuzzy digital object, fuzzy distance is a metric for the support of the object. A dynamic programming-based algorithm is presented for computing FDT of a fuzzy digital object. It is shown that the algorithm terminates in a finite number of steps and when it does so, it correctly produces the FDT image.

This paper is organized as follows. Section 2 describes the theory and properties of FDT in both continuous and digital cubic spaces. The metric property of fuzzy distance is studied in the same section. A dynamic programming-based algorithm for computing FDT of digital objects is presented in Section 3. The termination of the algorithm in a finite number of steps as well as its correctness are established in the same section. The results of applications of the FDT method are presented in Section 4. Finally, the conclusions are drawn in Section 5.

2. THEORY

In this section, we formulate the theory and study the properties of fuzzy distance transform of fuzzy subsets defined either in the continuous space or in a digital space. First, we will describe the case for the continuous space which will then guide the formulation in a digital space.

2.1. FDT in Continuous Space

Let $\Re^n$ denote the n-dimensional continuous space. A *fuzzy subset* [5] $\mathcal{S}$ of $\Re^n$ is defined as a set of pairs $\{(x, \mu_{\mathcal{S}}(x)) \mid x \in \Re^n\}$ where $\mu_{\mathcal{S}} : \Re^n \to [0, 1]$ is the *membership function* of $\mathcal{S}$ in $\Re^n$. For any value $\theta \in [0, 1]$, *θ-support* of $\mathcal{S}$, denoted by $\Theta_\theta(\mathcal{S})$, is the hard subset $\{x \mid x \in \Re^n \text{ and } \mu_{\mathcal{S}}(x) \geq \theta\}$ of $\Re^n$. In other words, the θ-support of $\mathcal{S}$ is the set of all points in $\Re^n$ with membership values greater than or equal to θ. 0-support will often be referred to as *support* and be denoted by $\Theta(\mathcal{S})$. A fuzzy subset with a bounded support is called *bounded*.

The following notions on fuzzy subsets are used in this paper; see [27, 28] for details. A fuzzy subset $\mathcal{S}$ is a *ring* if $\mu_{\mathcal{S}}(x) = \tilde{\mu}(r)$, where $r = \|x - x_0\|$ for some $x_0 \in \Re^n$ and $\tilde{\mu} : \Re \to [0, 1]$ is a membership function. $\mathcal{S}$ is said to be *convex* if, for every three collinear points x, y, and z in $\Re^n$ such that y lies between x and z, $\mu_{\mathcal{S}}(y) \geq \min[\mu_{\mathcal{S}}(x), \mu_{\mathcal{S}}(z)]$. A convex ring is called a *fuzzy disk*. A fuzzy subset is called *smooth* if it is differentiable at every location $x \in \Re^n$.

Let S be a (hard) subset of $\Re^n$. We shall use $\bar{S}$ to denote its complement and *Interior* (S) to denote its interior, which is the largest open set contained in S. The distance transform (DT) of S may be represented as an image $\{(x, D_S(x)) \mid x \in \Re^n\}$ on $\Re^n$ where D_S is the DT value at x that is defined as follows.

$$D_S(x) = \inf\{\|x - y\| \mid y \in \bar{S}\}, \tag{2.1}$$

where, inf gives the infimum of a set of positive numbers and $\|\cdot\|$ is the Euclidean norm. In the above equation, S should be a proper subset of $\Re^n$. In digital images, we always deal with bounded objects so that $\bar{S}$ is always nonempty. In the subsequent discussions, we will consider the fuzzy distance transform of bounded subsets only.

Here, we define FDT of a fuzzy subset $\mathcal{S}$ in $\Re^n$. Similar to ordinary DT, FDT is an image on $\Re^n$; we shall denote the FDT image by a set of pairs $\{(x, \Omega_{\mathcal{S}}(x)) \mid x \in \Re^n\}$, where $\Omega_{\mathcal{S}}(x)$ is the FDT value at x which is defined in the following way.

A *path* π in $\Re^n$ from a point $x \in \Re^n$ to another point (not necessarily distinct) $y \in \Re^n$ is a continuous function $\pi : [0, 1] \to \Re^n$ such that $\pi(0) = x$ and $\pi(1) = y$. The *length* of a path π in $\mathcal{S}$, denoted by $\Pi_{\mathcal{S}}(\pi)$, is the value of the following integration

$$\Pi_{\mathcal{S}}(\pi) = \int_0^1 \mu_{\mathcal{S}}(\pi(t)) \left| \frac{d\pi(t)}{dt} \right| dt. \tag{2.2}$$

Following the above equation, $\Pi_{\mathcal{S}}(\pi)$ is the integral of membership values (in $\mathcal{S}$) along π. Note that, if we define the inverse path $\pi'(t) = \pi(1 - t)$ of π, it can be shown that $\Pi_{\mathcal{S}}(\pi) = \Pi_{\mathcal{S}}(\pi')$. A question arises at this point on weighting the path length using membership values. Although other membership-based weights, e.g., absolute derivatives, may be useful in some applications, we use membership values themselves as weights as we intend to define distance between two points as the minimum material that has be to be traversed through to proceed from one point to the other. Thus when a path passes through a low density (low membership) region, its length increases slowly and the portion of the path in the complement of the support of $\mathcal{S}$ contributes no length. This approach is useful to measure regional object depth, object thickness distribution, etc.

In some applications, it may be useful to consider lengths of connected paths (paths entirely contained in $\Theta(\mathcal{S})$) only. This can be conceived by incorporating a little change in the definition of path length as follows

$$\Pi'_{\mathcal{S}}(\pi) = \int_0^1 \mu'_{\mathcal{S}}(\pi(t)) \left| \frac{d\pi(t)}{dt} \right| dt, \tag{2.3}$$

where

$$\mu'_{\mathcal{S}}(x) = \begin{cases} \mu_{\mathcal{S}}(x), & \text{if } \mu_{\mathcal{S}}(x) > 0, \\ \infty, & \text{otherwise.} \end{cases} \tag{2.4}$$

It can be shown that both $\Pi_{\mathcal{S}}$ and $\Pi'_{\mathcal{S}}$ lead to identical FDT images and Theorems 2.4 and 2.5 (see later in this section), which originally proved $\Pi_{\mathcal{S}}$, are true for $\Pi'_{\mathcal{S}}$, also. In this paper, we use $\Pi_{\mathcal{S}}$ to define fuzzy distance.

The set of all paths from a point $x \in \Re^n$ to another point $y \in \Re^n$ is denoted by $\mathcal{P}(x, y)$. It may be noted that $\mathcal{P}(x, y)$ contains infinitely many paths. The shortest path from $x \in \Re^n$ to $y \in \Re^n$ in $\mathcal{S}$ is a path $\pi_{x,y} \in \mathcal{P}(x, y)$ such that $\Pi_{\mathcal{S}}(\pi_{x,y}) \leq \Pi_{\mathcal{S}}(\pi), \forall \pi \in \mathcal{P}(x, y)$. It is worth mentioning that there may or may not exist one shortest path between two points in a fuzzy subset and when it exists it may not be unique. Here, we describe a 2D example where no shortest path exists between two points. Let us consider a fuzzy subset of $\Re^2$ with its support as a disk and let us pick any two points x and y near its center. Within the support of the fuzzy subset, there are only two membership values—a high membership value for the points on the straight line segment joining x and y, and a low membership value elsewhere. It is not difficult to see that the straight line segment xy is not the shortest path between x and y and for any other path π between the two points it is possible to find a shorter path by further straightening the path. Although, the existence of one shortest path between two points in a fuzzy subset is not guaranteed, the infimum of path lengths always exists and is unique. Let $\zeta_{\mathcal{S}}(x, y)$ denote a subset of positive real numbers defined as $\zeta_{\mathcal{S}}(x, y) = \{\Pi_{\mathcal{S}}(\pi) \mid \pi \in \mathcal{P}(x, y)\}$; i.e., $\zeta_{\mathcal{S}}(x, y)$ is the set of all possible path lengths in $\mathcal{S}$ between x and y. The *fuzzy distance* from $x \in \Re^n$ to $y \in \Re^n$ in $\mathcal{S}$, denoted as $\omega_{\mathcal{S}}(x, y)$, is the infimum of $\zeta(x, y)$; i.e.,

$$\omega_{\mathcal{S}}(x, y) = \inf \zeta_{\mathcal{S}}(x, y). \tag{2.5}$$

In the following, we show that fuzzy distance satisfies metric properties.

LEMMA 2.1. *For any fuzzy subset $\mathcal{S}$ of $\Re^n$, fuzzy distance $\omega_{\mathcal{S}}$ satisfies the following properties for any $x, y \in \Re^n$,*

1. $\omega_{\mathcal{S}}(x, y) = 0, \quad$ *if* $x = y$,
2. $\omega_{\mathcal{S}}(x, y) = \omega_{\mathcal{S}}(y, x)$,
3. $\omega_{\mathcal{S}}(x, y) \leq \omega_{\mathcal{S}}(x, z) + \omega_{\mathcal{S}}(z, y), \quad$ *for any* $z \in \Re^n$.

Proof. To prove (1), we consider the path $\pi(t) = x$ for $t \in [0, 1]$. Following (2.2), the length $\Pi_{\mathcal{S}}(\pi)$ of the path is "0" as $|\frac{d\pi(t)}{dt}| = 0$ for $t \in [0, 1]$. Hence, (1) is proved.

Here, we prove (2). For any path π from x to y, there is one and only one path π' from y to x, where $\pi'(t) = \pi(1 - t)$. Following (2.2), it can be shown that $\Pi_{\mathcal{S}}(\pi) = \Pi_{\mathcal{S}}(\pi')$ and thus, $\zeta_{\mathcal{S}}(x, y) = \zeta_{\mathcal{S}}(y, x)$. Therefore, following (2.2), $\omega_{\mathcal{S}}(x, y) = \inf \zeta_{\mathcal{S}}(x, y) = \inf \zeta_{\mathcal{S}}(y, x) = \omega_{\mathcal{S}}(y, x)$. This completes the proof of (2).

Let z be any point in $\Re^n$. To prove (3), we shall show that for any small positive value δ, it is possible to construct a path from x to y whose length is less than $\omega_{\mathcal{S}}(x, z) + \omega_{\mathcal{S}}(z, y) + \delta$. Since, $\omega_{\mathcal{S}}(x, z)$ is the fuzzy distance between x and z in $\mathcal{S}$, for any small positive number ϵ, there exists a path from x to z whose length is less than $\omega_{\mathcal{S}}(x, z) + \epsilon$; let $\pi_{x,z}$ be a path between x and z such that $\Pi_{\mathcal{S}}(\pi_{x,z}) < \omega_{\mathcal{S}}(x, z) + \delta/2$. Similarly, we can show that there is a path $\pi_{z,y}$ from z to y such that $\Pi_{\mathcal{S}}(\pi_{z,y}) < \omega_{\mathcal{S}}(z, y) + \delta/2$. We can always construct a path $\pi : [0, 1] \to \Re^n$ between x and y by concatenating these two paths $\pi_{x,z}$ and $\pi_{z,y}$ as follows

$$\pi(t) = \begin{cases} \pi_{x,z}(2t), & \text{for } 0 \leq t \leq 0.5, \\ \pi_{z,y}(2t - 1), & \text{otherwise.} \end{cases}$$

Following (2.2),

$$\begin{aligned}\Pi_{\mathcal{S}}(\pi) &= \int_0^1 \mu_{\mathcal{S}}(\pi(t))\left|\frac{d\pi(t)}{dt}\right| dt \\ &= \int_0^1 \mu_{\mathcal{S}}(\pi_{x,z}(t))\left|\frac{d\pi_{x,z}(t)}{dt}\right| dt + \int_0^1 \mu_{\mathcal{S}}(\pi_{z,y}(t))\left|\frac{d\pi_{z,y}(t)}{dt}\right| dt \\ &= \Pi_{\mathcal{S}}(\pi_{x,z}) + \Pi_{\mathcal{S}}(\pi_{z,y}) \\ &< \omega_{\mathcal{S}}(x, z) + \omega_{\mathcal{S}}(z, y) + \delta.\end{aligned}$$

The above inequality is established for any small positive number δ and therefore, following that $\Pi_{\mathcal{S}}(\pi) \in \zeta_{\mathcal{S}}(x, y)$, the infimum of $\zeta_{\mathcal{S}}(x, y)$ is less than or equal to $\omega_{\mathcal{S}}(x, z) + \omega_{\mathcal{S}}(z, y)$. Hence $\omega_{\mathcal{S}}(x, y) \leq \omega_{\mathcal{S}}(x, z) + \omega_{\mathcal{S}}(z, y)$. Since, z can be any point in $\Re^n$, the proof of (3) is complete. ■

LEMMA 2.2. *For any fuzzy subset $\mathcal{S}$ of $\Re^n$, for any nonzero positive number $\theta \leq 1$, fuzzy distance $\omega_{\mathcal{S}}$ satisfies the following property for any $x, y \in \Re^n$ such that either x or y is in Interior*$(\Theta_\theta(\mathcal{S}))$,

$$\omega_{\mathcal{S}}(x, y) > 0, \qquad \text{if } x \neq y.$$

Proof. To prove the lemma, without loss of generality, let us assume that $x \in$ *Interior* $(\Theta_\theta(\mathcal{S}))$. Since $x \in$ *Interior*$(\Theta_\theta(\mathcal{S}))$ and x and y are two definite points, there exists a positive number δ such that the hyperball $B_{x\delta}$ with center at x and radius of δ is entirely contained in *Interior*$(\Theta_\theta(\mathcal{S}))$ and is disjoint from y. Therefore, any path π_{xy} from x to y must contain a subpath $\pi_{x\delta}$ from x to the boundary of $B_{x\delta}$ and the Euclidean length of $\pi_{x\delta}$ is at least δ. Let t be the infimum of the membership values over $B_{x\delta}$. It may be noted that there may not be the smallest membership value over $B_{x\delta}$ but there is always the infimum. Following the fact that $B_{x\delta} \subset$ *Interior*$(\Theta_\theta(\mathcal{S}))$, $t \geq \theta$. Therefore, following (2.2.), $\Pi_{\mathcal{S}}(\pi_{x,y}) \geq \Pi_{\mathcal{S}}(\pi_{x\delta}) \geq \delta\theta > 0$. Since $\pi_{x,y}$ is any path from x to y, the fuzzy distance $\omega_{\mathcal{S}}(x, y) \geq \delta\theta > 0$. ■

It is interesting to note that the above theorem is not true for $\theta = 0$. This can be demonstrated using a simple 2D example. Let us consider a fuzzy subset $\mathcal{S}$ with its support forming a disk centered at a point x. Let y be the point on the periphery of the disk at 0 radian angle with the horizontal axis emanating from x. The membership values are assigned over the disk as follows—all points in the disk within the angular interval $[0, \pi)$ (open at the upper end) around x are assigned 1; the points within the angular interval $[\pi, 1.5\pi)$ are assigned $1/2$; and so on. It is not difficult to see that, in this example, the fuzzy distance between the two distinct points $x \in$ *Interior*$(\Theta(\mathcal{S}))$ and y is 0.

In a smooth fuzzy subset $\mathcal{S}$, the membership values over a bounded closed region X inside $\Theta(\mathcal{S})$ have a nonzero infimum. The smoothness of $\mathcal{S}$ and the compactness of X together imply that the set of membership values over X includes all its limit values. Using this fact and the proof strategy of Lemma 2.2, the proof of the following lemma is straightforward.

LEMMA 2.3. *For any smooth fuzzy subset $\mathcal{S}$ of $\Re^n$, fuzzy distance $\omega_{\mathcal{S}}$ satisfies the following property for any $x, y \in \Re^n$ such that either x or y is in Interior*$(\Theta(\mathcal{S}))$,

$$\omega_{\mathcal{S}}(x, y) > 0, \qquad \text{if } x \neq y.$$

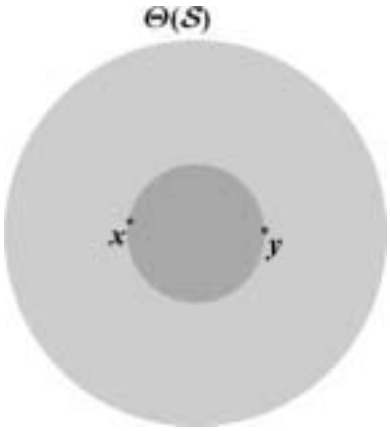

FIG. 1. An example demonstrating that the shortest paths (when they exist) between two points in a convex fuzzy subset are not necessarily a straight line segment. The support $\Theta(\mathcal{S})$ of the fuzzy disk is the union of different shaded regions. The points within the dark gray region have a sufficiently high membership value in $\mathcal{S}$ while the points within the light gray region have a sufficiently low membership value. Obviously, the shortest path between the two points x and y is contained within the light gray region and is not a straight line segment.

THEOREM 2.4. *For any fuzzy subset $\mathcal{S}$ of $\Re^n$, for any nonzero positive number $\theta \leq 1$, fuzzy distance $\omega_{\mathcal{S}}$ is a metric for Interior*$(\Theta_\theta(\mathcal{S}))$.

Proof. Obvious from Lemmas 2.1 and 2.2. ■

THEOREM 2.5. *For any smooth fuzzy subset $\mathcal{S}$ of $\Re^n$, fuzzy distance $\omega_{\mathcal{S}}$ is a metric for Interior*$(\Theta(\mathcal{S}))$.

Proof. Obvious from Lemmas 2.1 and 2.3. ■

It may be interesting to observe that the shortest paths (when they exist) in a fuzzy subset $\mathcal{S}$ between two points $x, y \in \Re^n$ are not necessarily a straight line segment even when $\mathcal{S}$ is convex. For example, consider the fuzzy disk $\mathcal{S}$ illustrated in Fig. 1. In the figure, the support $\Theta(\mathcal{S})$ of the fuzzy disk is the shaded region. In this example, within the support $\Theta(\mathcal{S})$, there are two possible membership values—points with high membership value are shown as dark gray and those with low membership value (within the outer annular region) are shown as light gray. Consider the two points x and y as illustrated in the figure. Assuming the high membership value sufficiently close to one and the low one close to zero, the shortest path between x, y should be contained within the light gray region and therefore is not a straight line segment.

Maintaining the same spirit as in the distance transform of hard sets, the FDT value $\Omega_{\mathcal{S}}(x)$ at a point $x \in \Re^n$ is equal to the fuzzy distance between x and the closest (with respect to $\omega_{\mathcal{S}}$) point in $\overline{\Theta(\mathcal{S})}$. In other words, the value of $\Omega_{\mathcal{S}}(x)$ is defined as follows

$$\Omega_{\mathcal{S}}(x) = \inf\{\omega_{\mathcal{S}}(x, y) \mid y \in \overline{\Theta(\mathcal{S})}\}. \tag{2.6}$$

2.2. FDT in Digital Cubic Spaces

Here, we describe fuzzy distance transformation in digital cubic spaces guided by the formulation of the same in the continuous space $\Re^n$ as discussed in the previous section. To make our description more precise, we will redefine the concepts in digital spaces which

we have already defined in the continuous space. In order to avoid unnecessary heaping of notations, we will use the same notations used in Section 2.1, although, their exact meaning in a digital space may be different from that in the continuous space.

A *digital space* $\mathcal{D}$ is an ordered pair (G, α) where G is the underlying digital grid and α is a binary relation on G that indicates the adjacency relationship between every two points in G. In general, a *digital grid* is a set of points in $\Re^n$ such that the interpoint distances are bounded below and within a bounded distance of any point in $\Re^n$ there is at least one point in the grid. However, most imaging systems acquire images in cubic grids and these grids are simple to describe as well as to understand. Therefore, we confine ourselves to cubic grids only. An n-dimensional cubic grid may be constructed by dividing $\Re^n$ into hypercuboids with n orthogonal families each of equally spaced parallel hyperplanes. The set of the centers of these hypercuboids generates a cubic grid and it is not difficult to see that, under a proper coordinate system, these points represent the points in Z^n where Z is the set of all integers. We use Z^n to represent an n-dimensional cubic grid. The notion of adjacency is useful to define a path in a digital space and the boundary of a digital object. Although researchers have used fuzzy adjacencies [29, 30], the interpretation of fuzziness of adjacencies in the context of a path is not clear. Therefore, we confine ourselves to hard adjacencies only. In other words, $\alpha : Z^n \times Z^n \to \{0, 1\}$. Two points $p, q \in Z^n$ are called *adjacent* if and only if $\alpha(p, q) = 1$. In the rest of this paper, α can be standard 4- or 8-adjacency in 2D, 6-, 18-, or 26-adjacency in 3D, and their higher dimensional analogs. Two adjacent points are often referred to as *neighboring* points to each other.

A *digital object* $\mathcal{O}$ is a fuzzy subset $\{(p, \mu_{\mathcal{O}}(p)) \mid p \in Z^n\}$, where $\mu_{\mathcal{O}} : Z^n \to [0, 1]$ specifies the membership value at each point in the object. It should be noted that, in general, an imaging system [31] acquires images containing information of a target object, often along with other co-objects. However, following the spirit of the problem addressed here, we start with the definition of digital objects instead of digital images [24]. In other words, the proposed framework assumes that the target object is already (fuzzily) segmented from an acquired digital image using an appropriate segmentation method [24, 32–34]. This process of extracting an object from an image, commonly referred to as image segmentation, has been studied extensively for decades. Since the subject itself is an open area of research, we prefer not to enter it here, but continue describing our theory assuming the above definition of a digital object. The support $\Theta(\mathcal{O})$ of a digital object $\mathcal{O}$ is the set of all points in Z^n each having a nonzero object membership value, i.e., $\Theta(\mathcal{O}) = \{p | p \in Z^n \text{ and } \mu_{\mathcal{O}}(p) \neq 0\}$. A *path* π in a set S of points from a point $p \in S$ to another (not necessarily distinct) point $q \in S$ is a sequence of points $\langle p = p_1, p_2, \ldots, p_m = q \rangle$ such that $p_i \in S$ for all $1 \leq i \leq m$ and p_j is adjacent to p_{j+1} for all $1 \leq j < m$. The length of the path is m. Although only hard adjacency relations are considered to define a path, we believe that the Euclidean distance between two adjacent points should be used in a meaningful way in defining its length. A set of points S will be called *path connected* if and only if, for every two points $p, q \in S$, there is a path in S from p to q. $\mathcal{P}(p, q)$ will denote the set of all paths in Z^n from a point $p \in Z^n$ to another point $q \in Z^n$. For the purpose of defining the length of a path, we use the notion of a link and its length. A *link* is a path consisting of two points. The length of a link $\langle p, q \rangle$ in $\mathcal{O}$ may be defined in different ways, e.g., (1) $\max\{\mu_{\mathcal{O}}(p), \mu_{\mathcal{O}}(q)\} \times \|p - q\|$, (2) $\frac{1}{2}(\mu_{\mathcal{O}}(p) + \mu_{\mathcal{O}}(q)) \times \|p - q\|$, etc. It may be noted that in both examples, the length of a link has two components—one coming from the membership values at p and at q and the other from the distance between the two points. In this paper, we will follow the second choice for the length of a link. Theoretical requirements for a valid length function

for links are (1) the length of a link $\langle p, p\rangle$ is "0", (2) the length of the links $\langle p, q\rangle$ and $\langle q, p\rangle \mid p, q \in Z^n$ are equal, and (3) the length of a link $\langle p, q\rangle$, where $p \in \Theta(\mathcal{O})$ and $p \neq q$, is greater than zero. The *length* $\Pi_{\mathcal{O}}(\pi)$ of a path $\pi = \langle p = p_1, p_2, \ldots, p_m = q\rangle$ is the sum of the lengths of all links on the path, i.e.,

$$\Pi_{\mathcal{O}}(\pi) = \sum_{i=1}^{m-1} \frac{1}{2}(\mu_{\mathcal{O}}(p_i) + \mu_{\mathcal{O}}(p_{i+1})) \times \|p_i - p_{i+1}\|. \tag{2.7}$$

$\pi_{p,q} \in \mathcal{P}(p, q)$ is one *shortest path* from $p \in Z^n$ to $q \in Z^n$ in $\mathcal{O}$ if $\Pi_{\mathcal{O}}(\pi_{p,q}) \leq \Pi_{\mathcal{O}}(\pi)$, $\forall \pi \in \mathcal{P}(p, q)$. Unlike the case of the continuous case, one shortest path always exists between two points in a bounded digital fuzzy object.

PROPOSITION 2.6. *For any digital space $\mathcal{D} = (Z^n, \alpha)$, for any fuzzy object $\mathcal{O}$ on $\mathcal{D}$ with a bounded support, for any two points $p, q \in Z^n$, there exists one shortest path from p to q.*

Proof. Let us consider a path $\pi = \langle p_1, p_2, \ldots, p_i, p_{i_1}, p_{i_2}, \ldots, p_{i_l}, p_i, p_{i+1}, \ldots, p_m\rangle$ with a repetition at p_i forming a loop (a path with the common starting and finishing point). Obviously, the length of the path $\langle p_1, p_2, \ldots, p_i, p_{i+1}, \ldots, p_m\rangle$, obtained by removing the repetition, is less than or equal to that of π. Therefore, to prove this proposition, we show that among the paths without any repetition, there is one with the smallest length. Since the support of $\mathcal{O}$ is bounded, there are only finitely many links with nonzero values and therefore, there are finitely many length values for the paths without any repetition. Hence, there is the minimum length for the paths between p and q and a path with the minimum length is one shortest path. ■

Although, the existence of one shortest path is guaranteed in fuzzy digital objects, as in the continuous space, there may be multiple shortest paths between two points in a fuzzy digital object between two points. In the rest of this paper, we consider fuzzy digital objects with bounded supports. The fuzzy distance, from $p \in Z^n$ to $q \in Z^n$ in $\mathcal{O}$, denoted as $\omega_{\mathcal{O}}(p, q)$, is the length of any shortest path in $\mathcal{O}$ from p to q. Therefore,

$$\omega_{\mathcal{O}}(p, q) = \min_{\pi \in \mathcal{P}(p,q)} \Pi_{\mathcal{O}}(\pi). \tag{2.8}$$

In the following, we show that, similar to the case of fuzzy subsets in the continuous space, fuzzy distance in a digital object defined over a digital cubic space is a metric.

LEMMA 2.7. *For any digital cubic space $\mathcal{D} = (Z^n, \alpha)$, for any digital object $\mathcal{O}$, fuzzy distance $\omega_{\mathcal{O}}$ satisfies the following properties for any $p, q \in Z^n$,*

1. $\omega_{\mathcal{O}}(p, q) = 0$, *if* $p = q$,
2. $\omega_{\mathcal{O}}(p, q) = \omega_{\mathcal{O}}(q, p)$,
3. $\omega_{\mathcal{O}}(p, q) \leq \omega_{\mathcal{O}}(p, r) + \omega_{\mathcal{O}}(r, q)$, *for any* $r \in Z^n$.

Proof. The strategy of the proof for this lemma is similar to that of Lemma 2.1. To prove (1), we consider the path $\langle p, p\rangle$ from p to p itself. Following (2.7), the length $\Pi_{\mathcal{O}}(\langle p, p\rangle) = \mu_{\mathcal{O}}(p) \times \|p - p\| = 0$. Hence, (1) is proved.

We prove (2) as follows. For any path $\pi = \langle p = p_1, p_2, \ldots, p_m = q\rangle$ from p to q, we can construct one and only one path π' from q to p as follows: $\pi' = \langle q = p_m, p_{m-1}, \ldots, p_1 = p\rangle$. It is not difficult to see that, following (2.7), $\Pi_{\mathcal{O}}(\pi) = \Pi_{\mathcal{O}}(\pi')$. Therefore, following (2.8), $\omega_{\mathcal{O}}(p, q) = \min_{\pi \in \mathcal{P}(p,q)} \Pi_{\mathcal{O}}(\pi) = \min_{\pi' \in \mathcal{P}(q,p)} \Pi_{\mathcal{O}}(\pi') = \omega_{\mathcal{O}}(q, p)$. This completes the proof of (2).

Here, we prove (3) by considering any point r in Z^n and assuming that $\pi_{p,r} = \langle p = p_1, p_2, \ldots, p_{m_p} = r\rangle$ is one shortest path from p to r while $\pi_{r,q} = \langle r = q_1, q_2, \ldots, q_{m_q} = q\rangle$ is one shortest path from r to q. Since, $p_{m_p} = q_1 = r$, we can concatenate these two paths $\pi_{p,r}$ and $\pi_{r,q}$ to construct a new path $\pi = \langle p = p_1, p_2, \ldots, p_{m_p}, q_2, \ldots, q_{m_q} = q\rangle$ from p to q. Following (2.7),

$$\begin{aligned}\Pi_{\mathcal{O}}(\pi) &= \sum_{i=1}^{m_p-1} \frac{1}{2}(\mu_{\mathcal{O}}(p_i) + \mu_{\mathcal{O}}(p_{i+1})) \times \|p_i - p_{i+1}\| \\ &\quad + \sum_{i=1}^{m_q-1} \frac{1}{2}(\mu_{\mathcal{O}}(q_i) + \mu_{\mathcal{O}}(q_{i+1})) \times \|q_i - q_{i+1}\| \\ &= \Pi_{\mathcal{O}}(\pi_{p,r}) + \Pi_{\mathcal{O}}(\pi_{r,q}) \\ &= \omega_{\mathcal{O}}(p, r) + \omega_{\mathcal{O}}(r, q).\end{aligned}$$

Obviously, $\pi \in \mathcal{P}(p, q)$ so that $\omega_{\mathcal{O}}(p, q) = \min_{\pi' \in \mathcal{P}(p,q)} \Pi_{\mathcal{O}}(\pi') \leq \Pi_{\mathcal{O}}(\pi) = \omega_{\mathcal{O}}(p, r) + \omega_{\mathcal{O}}(r, q)$. Since, r can be any point in Z^n, the proof of (3) is complete. ■

LEMMA 2.8. *For any digital cubic space $\mathcal{D} = (Z^n, \alpha)$, for any digital object $\mathcal{O}$, fuzzy distance $\omega_{\mathcal{O}}$ satisfies the following property for any $p, q \in Z^n$ such that either p or q is in $\Theta(\mathcal{O})$,*

$$\omega_{\mathcal{O}}(p, q) \neq 0, \qquad \text{if } p \neq q.$$

Proof. The strategy of the proof for this lemma is similar to that of Lemma 2.2. Without loss of generality, let us assume that $p \in \Theta(\mathcal{O})$. Let $\pi_{p,q}$ be a shortest path between p and q. Let r be the first point that follows p on $\pi_{p,q}$ but is not identical to p. Since, $p \neq q$, this assumption is always valid. Following (2.7), $\Pi_{\mathcal{O}}(\pi_{p,q}) \geq \frac{1}{2}(\mu_{\mathcal{O}}(p) + \mu_{\mathcal{O}}(r)) \times \|p - r\|$. Since $p \neq r$, $\|p - r\| > 0$. Again, since $p \in \Theta(\mathcal{O})$, $\mu_{\mathcal{O}}(p) > 0$ and obviously, $\mu_{\mathcal{O}}(r) \geq 0$. Therefore, $\frac{1}{2}(\mu_{\mathcal{O}}(p) + \mu_{\mathcal{O}}(r)) \times \|p - r\| > 0$. Hence, $\omega_{\mathcal{O}}(p, q) = \Pi_{\mathcal{O}}(\pi_{p,q}) > 0$. ■

THEOREM 2.9. *For any digital cubic space $\mathcal{D} = (Z^n, \alpha)$, for any digital object $\mathcal{O}$, fuzzy distance $\omega_{\mathcal{O}}$ is a metric for $\Theta(\mathcal{O})$.*

Proof. Obvious from Lemmas 2.7 and 2.8. ■

Following the framework of FDT for fuzzy subsets in the continuous space, the FDT value at a point $p \in Z^n$ in a fuzzy object $\mathcal{O}$ over a digital space, denoted by $\Omega_{\mathcal{O}}(p)$, is equal to the fuzzy distance between p and the nearest point in $\overline{\Theta(\mathcal{O})}$. In other words, the value of $\Omega_{\mathcal{O}}(p)$ is defined as follows

$$\Omega_{\mathcal{O}}(p) = \min_{q \in \overline{\Theta(\mathcal{O})}} \omega_{\mathcal{O}}(p, q). \tag{2.9}$$

3. ALGORITHMS

In this section, we present an algorithm for computing the FDT of digital objects. Also, we will prove that the algorithm terminates in a finite number of steps and when it does so it outputs the FDT of the digital object. Assuming a uniform neighborhood, we can think that,

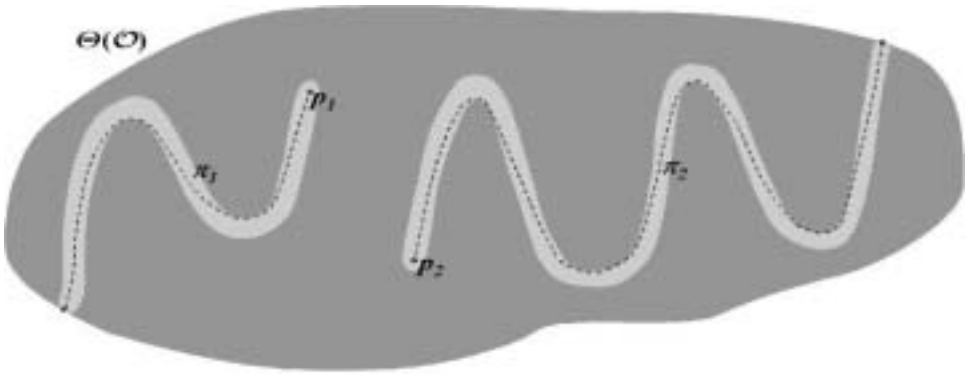

FIG. 2. An example demonstrating why a raster scan based approach fails to compute FDT for fuzzy digital objects in a fixed number of scans. The support $\Theta(\mathcal{O})$ of the fuzzy object $\mathcal{O}$ is the union of different shaded regions. The dark (light) gray region resembles the set of points with sufficiently high (respectively, low) membership values in $\mathcal{O}$. The path π_1 (π_2) is the shortest path in $\mathcal{O}$ from p_1 (respectively, p_2) to the complement of $\Theta(\mathcal{O})$. Computation of the length of π_1 (π_2), i.e., the FDT value at p_1 (respectively, at p_2) in $\mathcal{O}$, needs three (respectively, five) raster scans.

with respect to a point $p \in Z^n$, all its adjacent neighbors are ranked. A vector δ, called a *resolution vector*, is used whose ith element gives the continuous distance between a point and its ith adjacent neighbor. Here, we use the $(3^n - 1)$-adjacency relation (i.e., 8-adjacency in 2D and 26-adjacency in 3D). Therefore, δ is a $(3^n - 1)$-dimensional vector. The information about the resolution vector δ may be directly obtained from the application imaging system. Let $N^*(p)$ denote the set of adjacent neighbors of a point $p \in Z^n$ excluding p itself.

As demonstrated in [4], a raster scan approach effectively computes regular DT for binary images using only two scans. A basic reason behind this is the fact that, in a binary image, the shortest path from a point to the background (the complement of the binary object) is always a straight line segment (in a digital sense). However, this is not true for fuzzy digital objects (see Fig. 2). This makes a raster scan based approach inappropriate in computing FDT. Here, we illustrate this using an example illustrated in Fig. 2. Similar to the example in Fig. 1 , in Fig. 2, dark gray indicates high membership in the object $\mathcal{O}$ and light gray indicates low membership. Let us consider two points p_1 and p_2 as shown in the figure. Let π_1 be a shortest path from p_1 to $\overline{\Theta(\mathcal{O})}$ and let π_2 be the same but from p_2. It is not difficult to see that three raster scans are needed to compute the length of π_1 in $\mathcal{O}$ (i.e., the FDT value at p_1) while it takes five scans to do so for π_2 (i.e., the FDT value at p_2). Therefore, the number of raster scans needed to compute the FDT of a fuzzy object is dependent on the shape of the object as demonstrated in Fig. 2. The iterative algorithm [24] for computing the distance transform of a hard digital object can be used to compute FDT of fuzzy objects. However, such approaches will be inefficient in this application as the shortest path from a point to the background may be quite complicated and for each iteration the method needs to scan the entire image.

In the following, we present a dynamic programming-based algorithm to compute FDT of a fuzzy digital object. Before we do so, we discuss a basic problem associated with DT in a cubic grid and present a solution to it. For the ease of illustration, we will describe the problem in 2D, although it is valid in multidimensional spaces. Let us take two simple examples as shown in Figs. 3a and 3b—one is a vertical bar with two pixel thickness and the other is the same but with three pixel thickness. The object points are shown by black

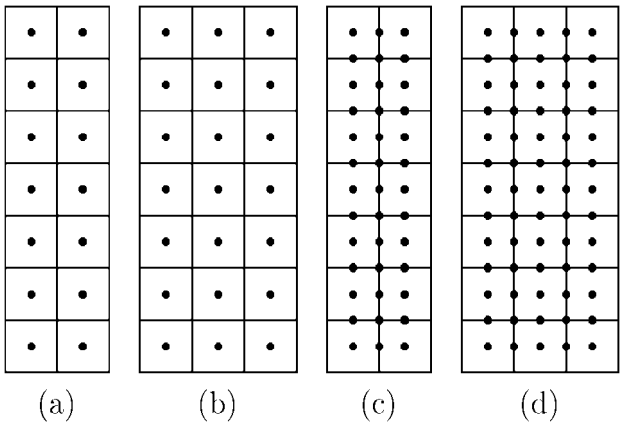

FIG. 3. An example illustrating a problem in DT-based thickness computation due to an even and odd number of digital points across the medial axis. (a, b) Two- and three-pixel thick vertical bars. Object points are shown by bullets. (c, d) Digital bars after halving resolution along each coordinate axis. Here too, object points are shown by bullets. Boundary points are shown by light gray bullets. A zero FDT value is assigned at every boundary point.

bullets. The largest DT value along a horizontal line is one for the case of Fig. 3a and it is two for Fig. 3b. This gives a thickness of two and four for Figs. 3a and 3b, respectively! This inaccuracy may have significant importance for applications with low thickness relative to image resolution. We present a solution to this problem as follows. Let $\mathcal{O} = (Z^n, \mu_{\mathcal{O}})$ be the fuzzy object under consideration. We construct a fuzzy digital object $\mathcal{O}' = (Z^n, \mu_{\mathcal{O}'})$ from $\mathcal{O}$ as follows.

Step A1. $\mu_{\mathcal{O}'}(2i+1, 2j+1) = \mu_{\mathcal{O}}(i, j)$ for all $i, j \in Z^n$. Let us call the points in $\mathcal{O}'$ with coordinates of the form $(2i+1, 2j+1)$ *primary point*s and among those, let us call the points with nonzero membership *primary object point*s.

Step A2. For a non-primary point $p \in Z^n$, if p is adjacent to a primary non-object point, assign $\mu_{\mathcal{O}'}(p) = 0$, otherwise assign $\mu_{\mathcal{O}'}(p) =$ the mean of the membership of all adjacent primary object points.

Finally, the resolution vector δ is updated accordingly and a zero FDT value is assigned at all points in $\overline{\Theta(\mathcal{O}')}$. When we apply the above two steps on a binary digital object (i.e., $\mu_{\mathcal{O}} : Z^n \to \{0, 1\}$) of Figs. 3a and 3b, we obtain the objects shown in Figs. 3c and 3d, respectively. It can be checked that DT-based thickness provides the correct results in both cases. In the following we present an algorithm to compute FDT.

ALGORITHM. *Compute_FDT*.

Input: $\mathcal{O} = (Z^n, \mu_{\mathcal{O}})$, α, and δ as defined in Section 2.
Auxiliary Data Structures: modified fuzzy object $\mathcal{O}' = (Z^n, \mu_{\mathcal{O}'})$, an image (Z^n, Ω) representing FDT of $\mathcal{O}'$, and a queue Q of points.
Output: an image (Z^n, Ω) representing FDT of $\mathcal{O}'$.

1. compute $\mathcal{O}' = (Z^n, \mu_{\mathcal{O}'})$ from $\mathcal{O} = (Z^n, \mu_{\mathcal{O}})$ following Steps A1 and A2;
2. for all $p \in \overline{\Theta(\mathcal{O}')}$, set $\Omega(p) = 0$;
3. for all $p \in \Theta(\mathcal{O}')$, set $\Omega(p) = MAX$;
   /* *MAX* is a large value */

4. for all $p \in \Theta(\mathcal{O}')$ such that $N^*(P) \cap \overline{\Theta(\mathcal{O}')}$ is non-empty
5. push p into Q;
6. *while* Q is not empty *do*
7. remove a point p from Q;
8. find $dist_{\min} = \min_{q \in N^*(p)}[\Omega(q) + \delta_{rank(p,q)} \times \frac{1}{2}(\mu_{\mathcal{O}'}(p) + \mu_{\mathcal{O}'}(q))]$;
/* $rank(p, q)$ gives the rank of q in the neighborhood of p */
9. *if* $dist_{\min} < \Omega(p)$ *then*
10. set $\Omega(p) = dist_{\min}$;
11. push all points $q \in N^*(p) \cap \Theta(\mathcal{O}')$ into Q;
12. output the FDT image $\mathcal{O}'$;

In the following two propositions, we prove that the algorithm *compute_FDT* terminates in a finite number of steps and when it does so it produces the FDT image.

PROPOSITION 3.1. *For any fuzzy object $\mathcal{O} = (Z^n, \mu_{\mathcal{O}})$ over any digital cubic space (Z^n, α), the algorithm compute_FDT terminates in a finite number of steps.*

Proof. The algorithm is iterative, and at each iteration in the *while-do* loop, it removes exactly one point from queue Q. Also, only the points of $\Theta(\mathcal{O}')$ visit Q. Since the number of elements in $\Theta(\mathcal{O}')$ is always finite, the algorithm *compute_FDT* fails to terminate in a finite number of steps only when some point $p \in \Theta(\mathcal{O}')$ is modified infinitely many times. Following Steps 9 and 10, the value at p strictly decreases after every modification. Moreover, following Steps 8, 9, and 10, during every modification, p is assigned the value of the length of some path in $\mathcal{O}'$ from p to a point in $\overline{\Theta(\mathcal{O}')}$. First, we show that p is always set to $\Pi_{\mathcal{O}'}(\pi)$ for some π without any repetition or loop. If this is not true, without loss of generality, let p be the first point to break the rule. Therefore, the path π is of the form $q_1, q_2, \ldots, p, \ldots, p$. But, this is possible only when p has previously been assigned the length of the path $\pi' = q_1, q_2, \ldots, p$. Following (2.7), it is obvious that $\Pi_{\mathcal{O}'}(\pi') \leq \Pi_{\mathcal{O}'}(\pi)$. But this contradicts Step 9. Now, since $\Theta(\mathcal{O}')$ is finite, there are only finitely many length values for repetition-free paths from $\overline{\Theta(\mathcal{O}')}$ to p (see the arguments in the proof of Proposition 2.3). Hence, any point $p \in Z^n$ could be modified only finitely many times. Hence *compute_FDT* terminates in a finite number of steps. ■

To prove the correctness of the algorithm we need the following notation. Let $T_{p,\overline{\Theta(\mathcal{O}')}}(l)$ denote the set of all paths of less than or equal to l points from p to some $q \in \overline{\Theta(\mathcal{O}')}$.

PROPOSITION 3.2. *For any fuzzy object $\mathcal{O} = (Z^n, \mu_{\mathcal{O}})$ over any digital cubic space (Z^n, α), when the algorithm compute_FDT terminates, its output equals the FDT image $(Z^n, \Omega_{\mathcal{O}'})$ of $\mathcal{O}'$ where $\mathcal{O}'$ is generated from $\mathcal{O}$ using Steps A1 and A2.*

Proof. Initially, the algorithm starts with the points of $\overline{\Theta(\mathcal{O}')}$ (see Steps 2–4). Thus, Steps 8–10 guarantee that whenever a point p is set to $dist_{\min}$ (in Step 10), there is always a path from some $q \in \overline{\Theta(\mathcal{O}')}$ to p with length $dist_{\min}$. Therefore, for any $p \in Z^n$, $\Omega(p) \geq \Omega_{\mathcal{O}'}(p)$.

It may be observed from the algorithm that it never increases the value of any $p \in Z^n$. We now prove that, for any $p \in Z^n$, $\Omega_{\mathcal{O}'}(p) \geq \Omega(p)$ by using the method of induction. Obviously, for any $p \in Z^n$, $T_{p,\overline{\Theta(\mathcal{O}')}}(1)$ is nonempty implies that $p \in \overline{\Theta(\mathcal{O}')}$, and following (2.7), the length of any element of $T_{p,\overline{\Theta(\mathcal{O}')}}(1)$ is always "0". Thus, in Step 2, it is guaranteed that the algorithm sets every point $p \in Z^n$ to the length of the shortest path of $T_{p,\overline{\Theta(\mathcal{O}')}}(1)$ in $\mathcal{O}'$. Now let us assume that the algorithm sets every point $p \in \Theta(\mathcal{O}')$ to the length of

the shortest path of $T_{p,\overline{\Theta(\mathcal{O}')}}(i-1)$, for some $i > 1$, in $\mathcal{O}'$. We show that the algorithm sets every point $p \in Z^n$ to the length of the shortest path of $T_{p,\overline{\Theta(\mathcal{O}')}}(i)$ in $\mathcal{O}'$ in Steps 7–11. Let $\pi_p = \langle q = p_1, p_2, \ldots, p_i = p \rangle$ be the shortest in $\mathcal{O}'$ among all paths of $T_{p,\overline{\Theta(\mathcal{O}')}}(i)$ from a point $q \in \overline{\Theta(\mathcal{O}')}$ to p. Following the hypothesis of the induction method, at a certain iteration the algorithm sets the point p_{i-1} to $\Omega(p_{i-1}) = \min_{\pi \in T_{p_{i-1},\overline{\Theta(\mathcal{O}')}}(i-1)} \Pi_{\mathcal{O}'}(\pi) \leq \Pi_{\mathcal{O}'}(\langle p_1, p_2, \ldots, p_{i-1} \rangle)$ at Step 10, and Step 11 ensures that, in the same iteration, p is pushed into Q; and upon the removal of p from Q, it is assigned (see Steps 7 to 10) a value less than or equal to $\Omega(p) = \Omega(p_{i-1}) + \delta_{rank(p_i, p_{i-1})} \times \frac{1}{2}(\mu_{\mathcal{O}'}(p_i) + \mu_{\mathcal{O}'}(p_{i-1})) \leq \Pi_{\mathcal{O}'}(\pi_p)$ (following (2.7); note that $\delta_{rank(p_i, p_{i-1})} = \| p_i - p_{i-1} \|$). Therefore, for any $p \in Z^n$, $\Omega_{\mathcal{O}'}(p) \geq \Omega(p)$. Hence, by the results in the previous paragraph, for any $p \in Z^n$, $\Omega_{\mathcal{O}'}(p) = \Omega(p)$. ■

4. RESULTS AND DISCUSSIONS

In this section, we present a few examples of the application of FDT methods presented in Sections 2 and 3 and will describe a method of computing local thickness using FDT in Section 4.1. The first example is a fuzzy object constructed from a 2D slice of a 3D computed tomographic angiography (CTA) image of a patient's head. The original slice is shown in Fig. 4a. The inplane resolution of the image is 0.25×0.25 mm^2. A fuzzy object was generated as follows. The bone regions were segmented from the slice image through interactive thresholding. The fuzzy object representing the bone region was constructed by (1) blurring (to simulate partial volume effects) the thresholded image over a Gaussian kernel of radius 5 pixels, and (2) subsequently adding a correlated, zero-mean Gaussian noise with standard deviation equal to 10% of the pixel bone fraction value. The final fuzzy object is shown in Fig. 4b. The motivation behind the construction of the fuzzy object in this way is simply to demonstrate the results on a relatively realistic image. Figure 4c shows the FDT image as derived from the fuzzy object of Fig. 4b. In Fig. 4c, the intensity values are proportional to its FDT value. As visually apparent in this figure, the ridges of FDT values follow the medial axis of the fuzzy object suggesting that there may be potential applications of FDT in computing skeletons of fuzzy objects.

4.1. Computation of Thickness

Thickness is a useful parameter in analyzing object shape and morphology. In this section, we briefly describe a method to compute thickness of a fuzzy object $\mathcal{O}$.

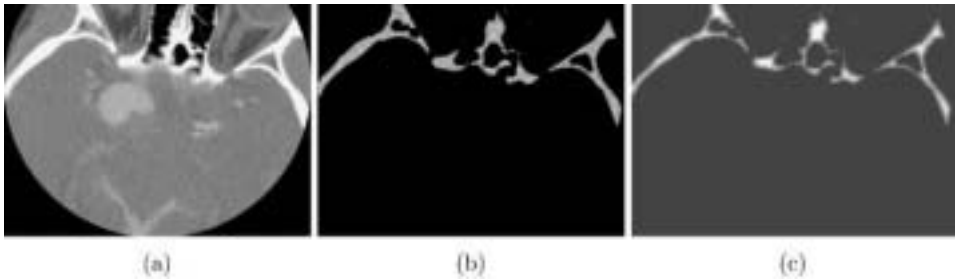

FIG. 4. Application of FDT on a fuzzy object. (a) A 2D slice from a 3D CTA image of a patient's head. (b) A fuzzy object representing the bone structures in (a). The fuzzy object was constructed from the image of (a) by first thresholding the bone regions and then by blurring and subsequently adding noise to it. (c) FDT image of the fuzzy object in (b). As visually appears in this figure, the ridges of FDT values follow the medial axis of the fuzzy object.

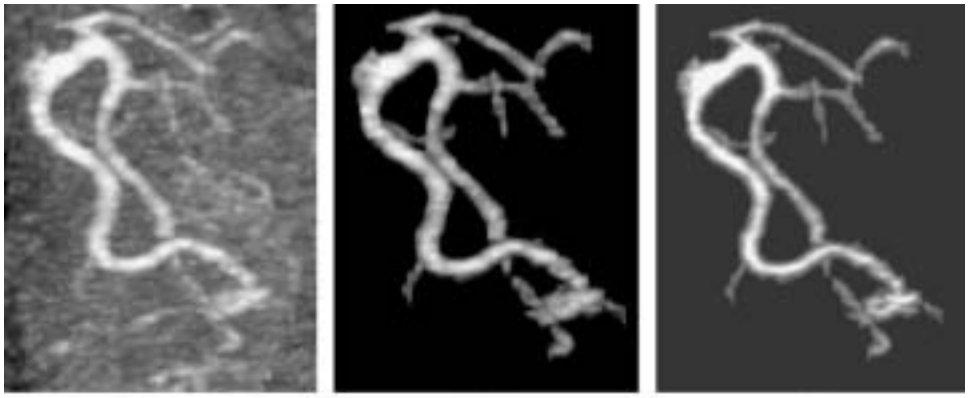

FIG. 5. Application of FDT-based thickness computation to an arterial tree. (a) A MIP rendering of a 3D subvolume taken from a 3D CTA image of a patient's head (after removing bones) showing a portion of the carotid arterial tree. (b) A MIP projection of the fuzzily segmented arterial tree. (c) A MIP projection of the FDT image of the 3D image shown in (b). Mean and standard deviation of thickness values computed along the curve skeleton of the arterial tree mask are 2.74 and 1.8 mm, respectively.

Thickness is computed along the medial surface of $\mathcal{O}$. Skeletonization [11–13] is widely used to generate the medial surface representation of a digital object. Following the same trend, we compute thickness along the skeleton of an object. It is desirable to generate the skeleton of an object directly from its fuzzy representation. However, this demands significant research and developments and is out of the support of the present paper. Therefore, we use the skeleton of the support $\Theta(\mathcal{O})$ of $\mathcal{O}$ to compute its thickness. For this purpose, we use the skeletonization method described in [13]. Let $Sk(\Theta(\mathcal{O}))$ denote the skeleton of $\Theta(\mathcal{O})$. At any point $p \in Sk(\Theta(\mathcal{O}))$, the thickness value is computed as twice the largest FDT value in the neighborhood of p.

The first example of FDT-based thickness computation is illustrated in Fig. 5. Figure 5a shows a maximum intensity projection (MIP) rendition of a portion of an arterial tree in a 3D CTA image of a subject's brain vasculature. The size of the image domain is $74 \times 217 \times 40$ and the voxel size is $0.32 \times 0.32 \times 1.25$ mm^3. The image has been rendered after removing bone using a recently developed method [36] in our laboratory. The mask for the arterial tree was segmented from the rest of the tissue using scale-based fuzzy connectedness [10]. A membership value $\mu_{\mathcal{A}}(p)$ at each location within the segmented artery mask was computed as

$$\mu_{\mathcal{O}}(p) = \begin{cases} G_{m_{\mathcal{A}},\sigma_{\mathcal{A}}}(f(p)), & \text{if } f(p) \le m_{\mathcal{A}}, \\ 1, & \text{otherwise,} \end{cases} \tag{4.1}$$

where f is the image intensity function, $m_{\mathcal{A}}$ and $\sigma_{\mathcal{A}}$ are mean and standard deviation of intensity values within the arterial mask and $G_{m_{\mathcal{A}},\sigma_{\mathcal{A}}}$ is an unnormalized Gaussian function with $m_{\mathcal{A}}$ and $\sigma_{\mathcal{A}}$ as its mean and standard deviation parameters. A zero membership value is assigned at each location outside the artery mask. A MIP rendition of the membership image of the arterial tree is presented in Fig. 5b. The FDT image was computed for the 3D membership image of the arterial tree and the MIP rendition of the FDT image is illustrated

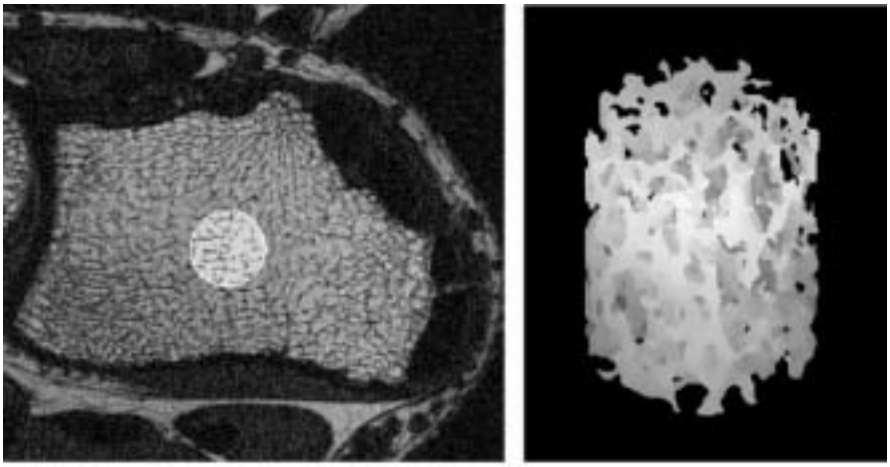

FIG. 6. Application of the FDT-based thickness computation method to high-resolution *in vivo* 3D MR images of the human distal radius showing trabecular bone structure. (a) A 2D slice taken from the raw 3D MR image. The central highlighted disk represents the cross section with the cylindrical ROI used for computing thickness of the bone trabeculae. (b) A 3D projection of the BVF image computed over the ROI. Mean and standard deviation of the thickness values of trabecular bone over the selected ROI are 102 and 42 μm, respectively, in good agreement with the known thickness of human bone trabecular which is on the order 100–150 μm [39].

in Fig. 5c. In order to compute thickness, a curve skeleton of the arterial tree was computed using the method in Saha *et al.* [13]. The mean and the standard deviation of thickness (vessel diameter) values along the skeleton were 2.74 and 1.8 mm, respectively. Arterial plaques can be detected by identifying sudden reduction of vessel diameter while tracing along the curve skeleton of an arterial tree.

The second example of thickness computation, illustrated in Fig. 6, is a high-resolution *in vivo* 3D magnetic resonance (MR) image of the human distal radius showing the trabecular bone network. The *in vivo* images were acquired on a 1.5T GE clinical scanner. The image size was $512 \times 256 \times 32$ and the voxel size was $137 \times 137 \times 350$ μm^3. A slice from the raw image is shown in Fig. 6a. A cylindrical region of interest (ROI) was chosen for analysis. The central highlighted disk in Fig. 6a is the cross section of the ROI with that slice. The image within the ROI was preprocessed by deshading and noise reduction using a histogram deconvolution method [37] to produce a bone volume fraction (BVF) map. The spatial resolution was enhanced to $68 \times 68 \times 88$ μm^3 using subvoxel classification [38]. A 3D projection of the final BVF image is presented in Fig. 6b. The FDT image was computed from the resolution-enhanced BVF image. Thickness values were computed using a surface skeleton [13] of the bone mask. The mean and the standard deviation of thickness values along the skeleton were 102 and 42 μm, respectively.

A further demonstration of the effectiveness of the proposed FDT-based thickness computation method involving high-resolution micro-computed tomography (μ-CT) images is presented in Fig. 7. The basic idea was to evaluate the FDT-based thickness distributions over four regions, two each from the same trabecular bone sample. Two μ-CT images of different metaphyseal samples of human distal radius were acquired on a SANCO Medical μ-CT 20 scanner at 22 μm isotropic resolution. Each of the two μ-CT images was processed as follows. The raw gray-scale image was binarized to yield bone masks. A BVF map at

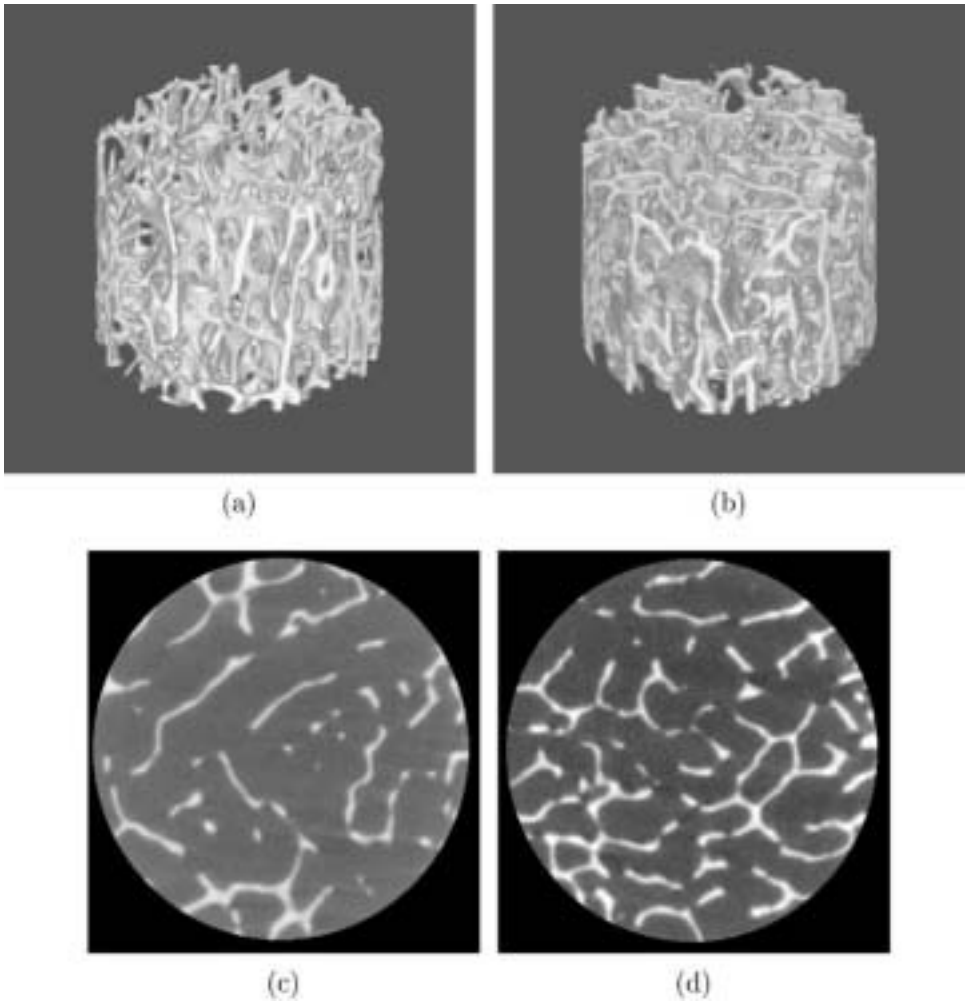

FIG. 7. Preliminary validation of FDT-based thickness method using μ-CT data of human distal radius trabecular bone by studying thickness distributions over four regions, two each from the same trabecular bone sample. (a, b) Fuzzy shell rendering of the 3D BVF image of trabecular bone networks for the two different specimens. (c, d) Two representative slices of the raw μ-CT image, one from each of the two samples shown in (a) and (b). (e) Two FDT-based thickness distributions, one from each of the two different slices (330 μm apart) chosen from the sample shown in (a). (f) Same as (e) but for the sample in (b).

each location within the bone mask was computed using an equation similar to (4.1). The BVF images of the two samples are illustrated in Figs. 7a and 7b using fuzzy shell rendering [40] supported by the 3DVIEWNIX [41] system. Two representative slices of the raw μ-CT images, one from each sample, are shown in Figs. 7c and 7d. A pair of slices, separated by 330 μm (i.e., 15 slices apart), was selected from each of the two samples and 2D FDT-based thickness was computed for each BVF slice image separately. Figure 7e shows two distributions of the thickness values, one for each of the two different slices chosen from the sample shown in Fig. 7a. The mean and standard deviations of thickness values in one slice were 119 and 59 μm, respectively, and the corresponding values for the other slice in the same sample were 116 and 62 μm, respectively. Figure 7f presents thickness distributions for the two slices chosen from the other sample shown in Fig. 7b. The mean and standard

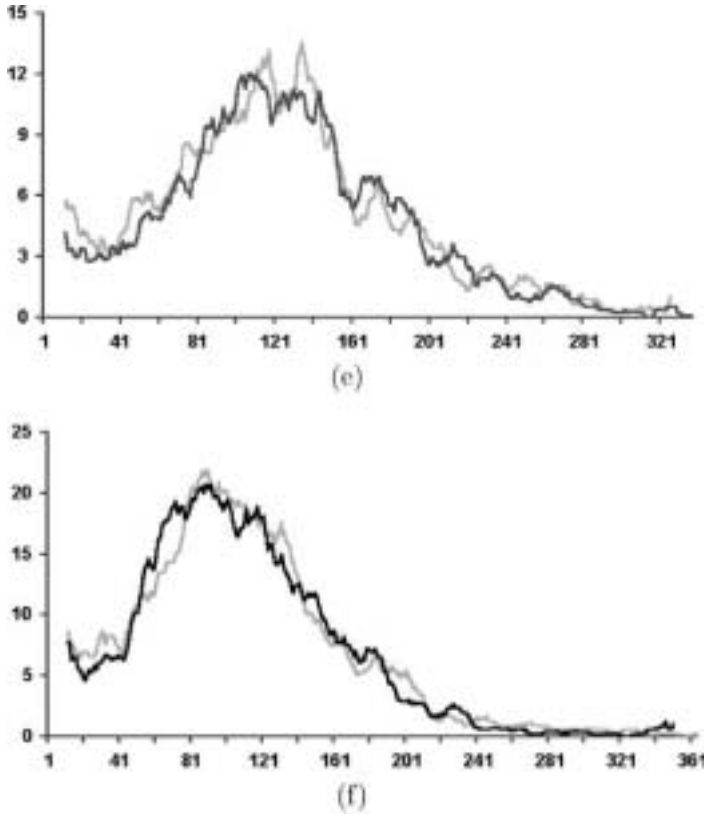

FIG. 7—*Continued*

deviations of thickness values in one slice are 103 and 57 μm, respectively, versus values for the other slice in the same sample of 101 and 54 μm, respectively. As demonstrated in Figs. 7e and 7f, the thickness distributions for the slices from the same sample are quite similar while they are significantly different for the pair of slices from the other sample. These observations are confirmed by the mean thickness values. These preliminary experiments show that the thickness value computed using the proposed methods is an intrinsic property of trabecular bone at a particular skeletal location and subject while these values may be quite different for corresponding locations in different subjects.

5. CONCLUSION

Theory and algorithms have been presented for fuzzy distance transforms representing an extension of the concept of distance transforms for hard objects to the more common fuzzy objects present in imaging. It has been shown that fuzzy distance is a metric for the interior of the support of a fuzzy object. A salient feature of fuzzy objects is the property that the shortest path between two points is no longer a straight line. It has also been shown that the raster scan algorithm commonly used for distance transforms of hard objects fails in the case of fuzzy objects. A dynamic programming-based algorithm has been presented for computing FDT of fuzzy digital objects. It has been shown that the algorithm terminates in a finite

number of steps and when it does so, it correctly computes FDT. Finally, several potential applications for fuzzy distance transforms in medical imaging are presented, including the quantification of the thickness of vascular structures and of trabecular bone. The method is likely to be of significant value for structural object analysis once the technique has been fully validated.

ACKNOWLEDGMENTS

This work was supported by NIH Grants RO1 41443 and R21 47112.

REFERENCES

1. A. Rosenfeld and J. Pfaltz, Distance functions in digital pictures, *Pattern Recog.* **1**, 1968, 33–61.
2. P. E. Danielsson, Euclidean distance mapping, *Comput. Graphics Image Process.* **14**, 1980, 227–248.
3. G. Borgefors, Distance transformations in arbitrary dimensions, *Comput. Vision Graphics Image Process.* **27**, 1984, 321–345.
4. G. Borgefors, On digital distance transformation in three dimensions, *Comput. Vision Image Understanding* **64**, 1996, 368–376.
5. A. Kaufmann, *Introduction to the Theory of Fuzzy Subsets*, Vol. 1, Academic Press, New York, 1975.
6. A. Rosenfeld, Fuzzy digital topology, *Inform. Control* **40**, 1979, 76–87.
7. J. C. Bezdek and S. K. Pal, *Fuzzy Models for Pattern Recognition*, IEEE Press, New York, 1992.
8. K. S. Fu and A. Rosenfeld, Pattern recognition and image processing, *IEEE Trans. Comput.* **25**, 1976, 1336–1346.
9. S. M. Pizer, D. Eberly, D. S. Fritsch, and B. S. Morse, Zoom-invariant vision of figural shape: The mathematics of cores, *Comput. Vision Image Understanding* **69**, 1998, 55–71.
10. P. K. Saha, J. K. Udupa, and D. Odhner, Scale-based fuzzy connected image segmentation: Theory, algorithms, and validation, *Comput. Vision Image Understanding* **77**, 2000, 145–174.
11. S. N. Srihari and J. K. Udupa, Understanding the bin of parts, in *Proceedings of International Conference on Cybernetics and Society, Denver, Colorado, 1979*, pp. 44–49.
12. Y. Tsao and K. S. Fu, A parallel thinning algorithm for 3D pictures, *Comput. Graphics Image Process.* **17**, 1981, 315–331.
13. P. K. Saha, B. B. Chaudhuri, and D. Dutta Majumber, A new shape preserving parallel thinning algorithm for 3D digital images, *Pattern Recog.* **30**, 1997, 1939–1955.
14. T. Serra, *Image Analysis and Mathematical Morphology*, Academic Press, San Diego, 1982.
15. G. Borgefors, Applications of distance transformations, in *Aspects of Visual Form Processing* (C. Arcelli *et al.*, Eds.), pp. 83–108, World Scientific, Singapore, 1994.
16. A. Rosenfeld and J. Pfaltz, Sequential operations in digital picture processing, *J. Assoc. Comput. Mach.* **13**, 1966, 471–494.
17. N. Okabe, J. Toriwaki, and T. Fukumura, Paths and distance functions in three dimensional digitized pictures, *Pattern Recog. Lett.* **1**, 1983, 205–212.
18. I. Ragnemalm, The Euclidean distance transform in arbitrary dimensions, *Pattern Recog. Lett.* **14**, 1993, 883–888.
19. G. Borgefors, Distance transformations in digital images, *Comput. Vision Graphics Image Process.* **34**, 1986, 344–371.
20. B. J. H. Verwer, Local distances for distance transformations in two and three dimensions, *Pattern Recog. Lett.* **12**, 1991, 671–682.
21. A. L. D. Beckers and A. W. M. Smeulders, Optimization of length measurements for isotropic distance transformations in three dimensions, *CVGIP: Image Understanding* **55**, 1992, 296–306.

22. D. Rutovitz, Data structures for operations on digital images, in *Pictorial Pattern Recognition* (G. C. Cheng *et al.*, Eds.), pp. 105–133, Thompson, Washington, DC, 1968.
23. G. Levi and U. Montanari, A gray-weighted skeleton, *Inform. and Control* **17**, 1970, 62–91.
24. A. Rosenfeld and A. C. Kak, *Digital Picture Processing*, 2nd ed., Vol. 2, Academic Press, New York, 1982.
25. J. Mordeson and P. Nair, *Fuzzy Graphs and Fuzzy Hypergraphs*, Physica-Verlag, Berlin, 2000.
26. E. W. Weisstein, *CRC Concise Encyclopedia of Mathematics*, Chapman & Hall/CRC, Boca Raton, FL, 1999.
27. A. Rosenfeld, The diameter of a fuzzy set, *Fuzzy Sets Systems* **13**, 1984, 241–246.
28. A. Bogomolny, On the perimeter and area of fuzzy sets, *Fuzzy Sets Systems* **23**, 1987, 257–269.
29. A. Rosenfeld, The fuzzy geometry of image subsets, *Pattern Recog. Lett.* **2**, 1991, 311–317.
30. J. K. Udupa and S. Samarasekera, Fuzzy connectedness and object definition: theory, algorithms, and applications in image segmentation, *Graphical Models Image Process.* **58**, 1996, 246–261.
31. Z. H. Cho, J. P. Jones, and M. Sing, *Foundations of Medical Imaging*, Wiley, New York, 1993.
32. N. R. Pal and S. K. Pal, A review of image segmentation techniques, *Pattern Recog.* **26**, 1993, 1277–1294.
33. J. K. Udupa and G. T. Herman (Eds.), *3D Imaging in Medicine*, CRC Press, Boca Raton, FL, 1991.
34. M. Sonka, V. Hlavac, and R. Boyle, *Image Processing, Analysis, and Machine Vision*, 2nd ed., PWS Publishing, Brooks/Cole, Pacific Grove, CA, 1999.
35. T. Y. Kong, A. W. Roscoe, and A. Rosenfeld, Concepts of digital topology, *Topology Appl.* **46**, 1992, 219–262.
36. P. K. Saha, J. K. Udupa, and J. M. Abrahams, Automatic bone-free rendering of cerebral aneurysms via 3D-CTA, in *Proceedings of SPIE: Medical Imaging, San Diego, CA*, Vol. 4322, pp. 1264–1272, 2001.
37. S. N. Hwang and F. W. Wehrli, Estimating voxel volume fraction of trabecular bone on the basis of magnetic resonance images acquired in vivo, *Internat. J. Imaging Systems Tech.* **10**, 1999, 186–198.
38. Z. Wu, H. Chung, and F. W. Wehrli, A Bayesian approach to subvoxel tissue classification in NMR microscopic images of trabecular bone, *Magnetic Res. Med.* **31**, 1994, 302–308.
39. J. E. Aaron, N. B. Makins, and K. Sagreiya, The microanatomy of trabecular bone loss in normal aging men and women, *Clinical Orthopaedics Related Res.* **215**, 1987, 260–271.
40. J. K. Udupa and D. Odhner, Shell rendering, *IEEE Comput. Graphics Appl.* **13**(6), 1993, 58–67.
41. J. K. Udupa, D. Odhner, S. Samarasekera, R. J. Goncalves, K. Iyer, K. Venugopal, and S. Furuie, 3DVIEWNIX: A open, transportable, multidimensional, multimodality, multiparametric imaging system, Proc. *SPIE* **2164**, 1994, 58–73.